Calcium Is Essential for the Structural Integrity of the Cysteine-Rich, Ligand-Binding Repeat of the Low-Density Lipoprotein Receptor†

Annette R. Atkins,‡ Ian M. Brereton,§ Paulus A. Kroon,‡ Huang T. Lee,‡ and Ross Smith*,‡

Department of Biochemistry and Centre for Magnetic Resonance, University of Queensland, Queensland 4072, Australia

Received October 13, 1997; Revised Manuscript Received November 25, 1997

ABSTRACT: Seven cysteine-rich repeats form the ligand-binding region of the low-density lipoprotein (LDL) receptor. Each of these repeats is assumed to bind a calcium ion, which is needed for association of the receptor with its ligands, LDL and β-VLDL. The effects of metal ions on the folding of the reduced N-terminal cysteine-rich repeat have been examined by using reverse-phase high-performance liquid chromatography to follow the formation of fully oxidized isomers with different disulfide connectivities. In the absence of calcium many of the 15 possible isomers formed on oxidation, whereas in its presence the predominant product at equilibrium had the native disulfide bond connectivities. Other metals were far less effective at directing disulfide bond formation: Mn^{2+} partly mimicked the action of Ca^{2+}, but Ba^{2+}, Sr^{2+}, and Mg^{2+} had little effect. This metal-ion specificity was also observed in two-dimensional ^{1}H NMR spectral studies; only Ca^{2+} induced the native three-dimensional fold. The two paramagnetic ions, Gd^{3+} and Mn^{2+}, and Cd^{2+} did not promote adoption of a well-defined structure, and the two paramagnetic ions did not displace calcium ions. The location of calcium ion binding sites in the repeat was also explored by NMR spectroscopy. The absence of chemical shift changes for the side chain proton resonances of Asp26, Asp36, and Glu37 from pH 3.9 to 6.8 in the presence of calcium ions and their proximal location in the NMR structures implicated these side chains as calcium ligands. Deuterium exchange NMR experiments also revealed a network of hydrogen bonds that stabilizes the putative calcium-binding loop.

The recycling low-density lipoprotein receptor (LDLR)[1] is responsible for the cellular uptake of cholesterol through the internalization of apolipoprotein B-100 (apoB-100)-containing and apoE-containing lipoproteins from the blood. Mutations in the LDLR are associated with familial hypercholesterolemia, in which the number of functional receptors is reduced, resulting in elevated concentrations of plasma LDL and cholesterol and in accelerated atherosclerosis.

This receptor, the archetype of the LDL receptor gene superfamily, is a large, multidomain protein with cytoplasmic, single membrane spanning, epidermal growth factor (EGF) precursor-like, and ligand-binding domains. The amino-terminal, extracellular ligand-binding domain is composed of seven cysteine-rich, imperfect repeats of ~40 amino acids, each of which contains six conserved cysteine residues and several conserved acidic and hydrophobic amino acids. We have previously characterized the first two ligand-binding repeats (LB1 and LB2) as autonomously folding domains containing three intrarepeat disulfide bonds with the connectivities Cys1−Cys3, Cys2−Cys5, and Cys4−Cys6 (*1*−*3*). These two modules obtained from bacterial expression (rLB1 and rLB2) were shown by ^{1}H NMR spectroscopy to have a similar fold: a β-hairpin structure followed by a series of turns (*1*, *4*).

Calcium ions are required for the biological activity of the LDLR; binding of the lipoprotein particles is eliminated in the presence of EDTA (*5*). The recognition of the first repeat, LB1, by a conformationally specific monoclonal antibody, IgG-C7, is also dependent on the presence of calcium (*6*). It has therefore been proposed that each of the seven cysteine-rich repeats binds calcium, which is essential for maintenance of their biologically active conformations (*6*, *32*). This proposal is supported by the identification of cysteine-rich repeats in other members of the LDLR superfamily, such as the very low density lipoprotein receptor (VLDLR) and the LDL receptor-related protein (LRP), and in functionally unrelated proteins, such as the complement proteins C8 and C9, which similarly require calcium for recognition by antibodies (*7*, *8*) or their ligands (*9*). It has been postulated that the calcium induces allosteric changes in the cysteine-rich repeats which expose the ligand-binding site (*9*). This proposal is supported by the observed conformational dependence on calcium ions of the ^{1}H NMR

† This work was supported by a grant to P.A.K., R.S., and I.M.B. from the Australian National Health and Medical Research Council.

* Address for correspondence: Dr. Ross Smith, Biochemistry Department, The University of Queensland, Qld 4072, Australia. Telephone: 61 7 3365 4627. Fax: 61 7 3365 4699. E-mail: ross@biosci.uq.edu.au.

‡ Department of Biochemistry.

§ Centre for Magnetic Resonance.

[1] Abbreviations: CD, circular dichroism; 2D, two-dimensional; HPLC, high-performance liquid chromatography; LB1, N-terminal cysteine-rich repeat of the LDL receptor; LB5, fifth cysteine-rich repeat of the LDL receptor; LDL, low-density lipoprotein; LDLR, low-density lipoprotein receptor; LRP, LDL receptor-related protein; NOE, nuclear Overhauser enhancement; NOESY, 2D nuclear Overhauser enhancement spectroscopy; rLB1, recombinant N-terminal cysteine-rich repeat of the LDL receptor; rmsd, root-mean-square deviation; TFA, trifluoroacetic acid; TOCSY, 2D total correlation spectroscopy; VLDL, very low density lipoprotein.

S0006-2960(97)02529-4 CCC: $15.00
Published on Web 01/22/1998

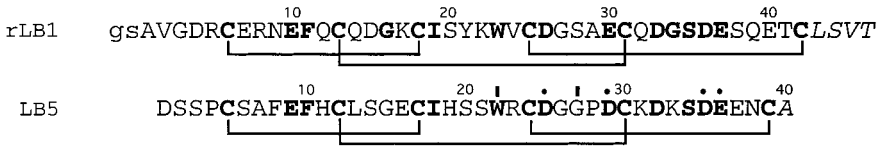

FIGURE 1: Sequences of rLB1 and LB5. Conserved residues across the ligand-binding repeats are shown in bold, the linker residues between repeats are in italics, and the two amino acid N-terminal extension from the GST fusion protein thrombin cleavage site of LB1 is in lowercase. Disulfide bonds are depicted by solid lines. Residues are numbered as for the native LB1 and as in Fass et al. for LB5 (*11*). Calcium-coordinating residues in LB5 are shown as circles and vertical bars for ligation through side-chain carboxylates and backbone carbonyls, respectively.

spectra of these repeats, where the well-dispersed spectra of the calcium-bound forms contrast with the broad, overlapped spectra obtained without metal (*4, 10*). Earlier indications (*1*) that the conformation of the first repeat was not influenced by calcium appear to be attributable to the presence of calcium in samples assumed to be calcium-free.

We have demonstrated here that calcium ions are required during the in vitro folding and oxidation of the first repeat; in the absence of calcium, a complex mixture of disulfide-bridged isomers is formed, while essentially complete folding to the wild-type conformation occurs with calcium present. The specificity of the ion-binding site for calcium was investigated by monitoring the in vitro folding of rLB1 in the presence of selected metal ions, and the ability of these ions to induce the native conformation in fully oxidized rLB1 was assessed from their effects on its two-dimensional ^{1}H NMR spectra. These studies indicated that the ion-binding site in the first repeat is specific for calcium. pH titration curves obtained for the acidic amino acids implicated particular residues in the calcium coordination which are in accord with the ligands identified from the crystal structure of the fifth repeat (*11*).

MATERIALS AND METHODS

Protein Expression. LB1 was expressed as a thrombin-cleavable glutathione S-transferase fusion protein that was cleaved and purified as described previously (*12*). The expressed peptide, rLB1, contains an extra glycine and serine on the N-terminus of the native LB1, and includes the four C-terminal residues corresponding to the linker between the first two repeats (Figure 1). The purified, oxidized peptide eluted as a single peak on analytical HPLC with the anticipated mass ($M = 5220$), as determined by electrospray ionization mass spectrometry.

Metal-free peptide solutions were prepared by dialyzing rLB1 extensively through 3000 molecular weight cutoff tubing against 1 mM EGTA, 1 mM EDTA, pH 6.0, and subsequently against water to remove the chelating agents. Typically, a sample volume of <1 mL was dialyzed at 4 °C against 1 L of chelating buffer for ~20 h with buffer changes every ~4 h and then under similar conditions against water. Calcium removal was confirmed by inspection of the amide region of the ^{1}H NMR spectrum, which lacked the dispersion seen in the native conformation.

Oxidation Experiments. rLB1 was reduced using excess dithiothreitol (~0.2 M) in 100 mM ammonium acetate, pH 8.3 at 37 °C for 1 h, and purified on a Vydac C18 analytical reverse-phase HPLC column (4.6 × 25 mm). Stock solutions at 25 mM were prepared from commercially supplied analytical grade metal chlorides for Ca^{2+}, Mg^{2+}, Mn^{2+}, Cd^{2+}, Gd^{3+}, Sr^{2+}, and Ba^{2+}. Aliquots of the reduced peptide were pre-equilibrated for 15 min at room temperature with 1 mM EGTA in 150 mM KCl, and then for a further 15 min with the selected metal ion. Disulfide bond formation was catalyzed by oxidized and reduced glutathione in Tris buffer at pH 7.3−7.6. The final concentrations in the oxidation reactions were: 6 μM peptide, 1 mM EGTA, 150 mM KCl, 2.5 mM metal chloride, 50 mM Tris, 3 mM reduced glutathione, and 0.3 mM oxidized glutathione. The metal ion aliquot was replaced with the equivalent volume of water for control experiments. The oxidation reactions were carried out at 4 °C and the products monitored at 1, 2, and 3 days by HPLC on a Vydac C18 analytical column with a gradient of 10−30% acetonitrile in 0.1% TFA over 40 min.

The extent of the oxidation reaction was established by treatment with the alkylating agent, 4-vinylpyridine. Excess, redistilled 4-vinylpyridine was reacted with the oxidation products, in 35% acetonitrile to maintain miscibility, for 2.5 h at pH ~8 and room temperature, and the products were compared with the starting material by reverse-phase HPLC.

NMR Experiments. ^{1}H NMR spectra were recorded on 0.6−1.5 mM peptide solutions in 10% ^2H_2O/90% H_2O using a Bruker DRX 500 spectrometer. TOCSY (*13*) and NOESY (*14*) spectra were recorded at 300 K. An MLEV-17 spin lock sequence of either 63 or 82 ms was employed in the TOCSY experiments and a 200-ms mixing time used NOESY spectra were collected. Time-proportional phase incrementation was utilized for quadrature detection in F1, and water suppression was accomplished with either pre-saturation or the WATERGATE sequence (*15*). Typically, spectra were recorded as 470−512 t_1 increments, collected into 4096 data points, and apodized using a 90° shifted sine-squared function in both dimensions within the Bruker software XWINNMR. Chemical shifts are referenced to internal 3-(trimethylsilyl)propionate (TSP) or 2,2-dimethyl-2-silapentane-5-sulfonic acid (DSS).

Adjustments to the pH of samples were made with small volumes of NaOH or HCl, and pH values are reported as the average of the reading before and after the experiment, without correction for the deuterium isotope effect. The pH readings typically differed by less than 0.1 pH units. Metal ions were added as aliquots from stock solutions of the chloride salts, and 100 mM KCl was added in experiments with the paramagnetic ions to minimize electrostatic interactions.

pK_a and pK_{app} values for the side-chain carboxylates and backbone amide protons were determined by fitting the ^{1}H chemical shift titration data to the Henderson−Hasselbalch equation.

Circular Dichroism Experiments. Circular dichroism (CD) spectra were recorded in a 1 mm path length cell at ambient temperature on a Jasco J-710 spectropolarimeter (Tokyo,

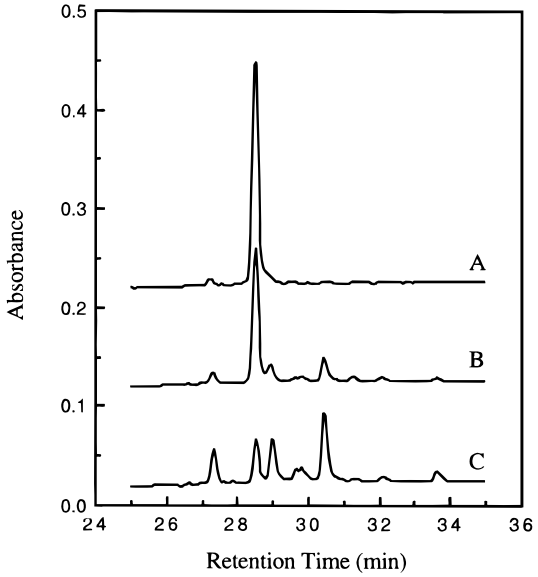

FIGURE 2: HPLC of the oxidation products for rLB1 folded in the presence of (A) 2.5 mM Ca^{2+}, (B) 2.5 mM Mn^{2+}, and (C) 1 mM EGTA, recorded at 214 nm. Reduced rLB1, oxidized for 3 days at 4 °C and pH 7.5, was analyzed on an analytical C18 column using a 10−30% CH_3CN/0.1% TFA gradient over 40 min.

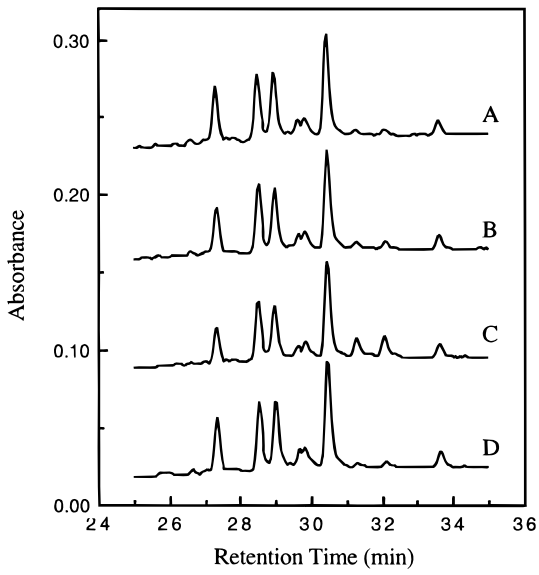

FIGURE 3: HPLC of the oxidation products of rLB1 folded in the presence of (A) 2.5 mM Ba^{2+}, (B) 2.5 mM Sr^{2+}, (C) 2.5 mM Mg^{2+}, and (D) 1 mM EGTA. Reaction and analysis conditions are as described in Figure 2.

Japan) using a bandwidth of 1.0 nm, a response time of 2 s, and a scan rate of 20 nm min^{-1}. Far UV spectra, recorded at 30 μM rLB1, were averaged over 3 scans between 250 and 200 nm and over 10 scans between 200 and 185 nm. Near-UV spectra were averaged over 10 scans across the wavelengths 320−250 nm at 230 μM rLB1. Spectra, recorded at pH 3 and 6 in the presence of either 1 mM calcium or 1 mM EDTA, were corrected for cell and solvent effects and are reported as mean residue ellipticities.

Hydrogen Bond Prediction. Hydrogen bonds were predicted for the fifth cysteine-rich repeat, LB5, from the coordinates deposited in the Brookhaven Protein Data Bank, accession code 1AJJ (*11*), using the Insight II program (Biosym/MSI, CA).

RESULTS

The Role of Ions During in Vitro Oxidation of rLB1. Oxidation of fully reduced rLB1 in the presence of 2.5 mM calcium ions gave one major peak on HPLC (Figure 2A) which coeluted with peptide known to be correctly folded, as judged by its ability to bind to the conformationally sensitive antibody, IgG-C7. The minor amounts of partially or incorrectly folded intermediates detected after 1 and 2 days were largely converted to the native conformation within 72 h.

In contrast, the oxidation of rLB1 in the absence of calcium yielded peptide that was resolved into many components on HPLC (Figure 2C). As the rLB1 was shown by electrospray mass spectroscopy to have the mass anticipated for the monomer and to be fully oxidized, as indicated by a lack of reactivity with 4-vinylpyridine, the multiple peaks may be ascribed to formation of many of the 15 possible isoforms resulting from intramolecular disulfide bond formation. In the absence of calcium, the component having the same HPLC retention time as the native isomer represented only ∼15% of the final, fully oxidized material. As the oxidation was performed at pH 7.3−7.6 in the presence of reduced and oxidized glutathione, conditions that facilitate free disulfide interchange, the final mixture of isoforms is likely to reflect their relative stabilities in the absence of metals.

The specificity of the ion-binding site was investigated by assessing the ability of selected divalent and trivalent cations to substitute for calcium in directing the formation of the disulfide bonds. As strontium and barium have been reported to facilitate receptor−ligand interaction of members of the LDLR superfamily in cell-based assays, their ability to influence the distribution of disulfide-bridged isomers was of interest. Although no metals other than calcium have been reported to activate the LDL receptor, cadmium, manganese, and ions from the lanthanide series have been demonstrated to bind to a variety of calcium-binding proteins with varying affinities. Thus, strontium, barium, cadmium, manganese, magnesium, and gadolinium have been added to the first repeat in the presence of redox buffers, and the oxidation products compared with those obtained in the presence of calcium by HPLC.

Oxidation in the presence of 2.5 mM manganese induced ∼60% of the peptide to form the native disulfide bonds, based on a comparison of the peak heights in the chromatograms (Figure 2B). Surprisingly, the oxidation products in the presence of strontium, barium, and magnesium were similar to those formed in the absence of any metal. Although minor differences were seen in the intensity of the late-eluting isomers, the relative intensities of the major products were very similar (Figure 3). Neither reduced nor oxidized peptide was observed after a 72-h reaction in the presence of either gadolinium or cadmium, suggesting that these metal ions precipitated the peptide or induced the formation of intermolecular disulfide bonds.

The oxidation of rLB1 in the absence of any redox buffers produced a distribution of isomers that was weakly dependent on the presence of calcium; a slight increase in the amount of native isomer was observed when calcium was present (Figure 4A). This is likely to result from slow disulfide interchange mediated by the reduced peptide. This finding suggests that the calcium influences the formation of

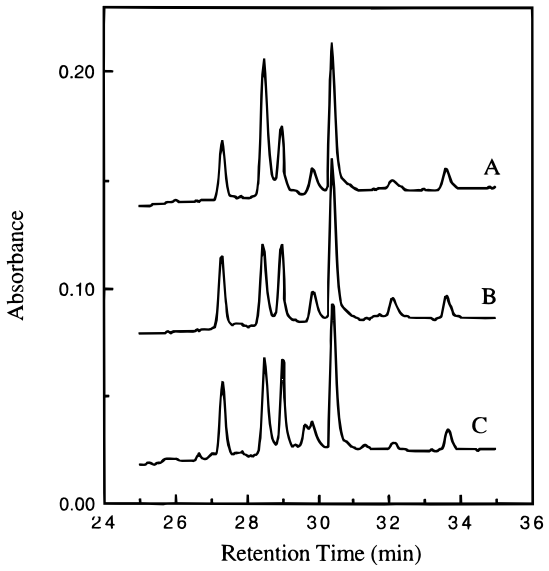

FIGURE 4: The effect of disulfide exchange on the distribution of isomers produced from the oxidation of rLB1. HPLC traces of the products of rLB1 folded in the presence of (A) 2.5 mM Ca^{2+} but no glutathione, (B) 1 mM EGTA but no glutathione, and (C) 1 mM EGTA and reduced and oxidized glutathione. Reaction and analysis conditions are as described in Figure 2.

disulfides by binding to, and preferentially stabilizing, the native isomer. This result is in accord with the general paradigm proposed for the formation of protein disulfide bonds in bovine pancreatic trypsin inhibitor (BPTI). In the presence of free thiols, initial BPTI folding is kinetically driven to form disulfide bonds between cysteines appropriately spaced in a linear sequence. These bonds then undergo intramolecular disulfide exchange causing the most stable isomer to accumulate (*16*). In the case of rLB1, the calcium appears to direct the formation of disulfide bonds by generating a more stable structure which is subsequently favored during disulfide exchange. It is implicit in this proposal that the fully reduced sequence of rLB1 does not bind calcium with high affinity. Similarly, calcium does not bind to either the unfolded form or the molten globule of α-lactalbumin, but binds to a transition state between the molten globule and the native isomer (*17*).

Calcium Dependence of the rLB1 Conformation. The calcium dependence of the conformation of rLB1 is readily observed in the ^1H NMR spectrum. In the presence of calcium at pH ∼6 the resonances were well-dispersed with amide signals spread across 3 ppm, facilitating sequence-specific assignments and subsequent structure calculations (Figure 5A). In calcium-free solutions, or at pH <4 in the presence or absence of Ca^{2+}, however, the notably downfield shifted amide resonances were absent, and the extensive overlap precluded complete assignment of the spectra (Figure 5B). The cross peaks were also broadened, consistent with conformational interchange. NMR spectra recorded with sub stoichiometric amounts of calcium revealed two sets of resonances for some residues, indicating that the calcium is in slow exchange on the time scale of the NMR experiments; an estimate of the upper limit of the exchange rate, based on the frequency difference of the calcium-bound and free resonances of C20 HN, is ∼26 s^{-1} (*18*).

Similar effects were seen in the CD spectra on the addition of calcium. The far-UV CD spectrum of rLB1 in the presence of 1 mM calcium at pH 6 displayed a weak positive band at 230 nm and a strong negative band at 200 nm (Figure 6A). The spectrum recorded in the absence of calcium (pH 3 and 1 mM EDTA, Figure 6A) was qualitatively similar, but no positive ellipticity was seen, and the intensity of the negative band at 200 nm was reduced to ∼60%. The spectrum recorded at pH 6 and 1 mM EDTA was essentially indistinguishable from that at pH 3, indicating that there were no secondary structural changes associated with the pH change (results not shown). The differences between the spectra are therefore attributable solely to the effects of calcium binding. This finding is contrary to earlier results where the addition of a stoichiometric amount of calcium did not affect the CD spectrum (*1*), and it is now thought that calcium was present as a contaminant in these earlier samples. In addition, the spectrum at pH 3 in the presence of 1 mM calcium is identical to the spectrum recorded in the absence of metal (results not shown), confirming the peptide's inability to bind calcium at low pH, as suggested by the NMR results at low pH (see above). This is consistent with carboxylate groups being involved in the coordination of the calcium.

Calcium-dependent structural changes were also observed in the near-UV CD spectrum, where ∼20% of the ellipticity was lost on removal of the calcium, suggesting that the packing of the aromatic side chains characteristic of a folded protein is dependent on the presence of calcium (Figure 6B).

Identification of the Calcium-Binding Site. The binding of the paramagnetic ions Mn^{2+} and Gd^{3+} to rLB1 was investigated in an attempt to map the Ca^{2+}-binding site. Mn^{2+} was unable to displace bound Ca^{2+}, however, as evidenced by the nonspecific relaxation of all resonances by 0.05 molar equiv, and 0.5 molar equiv did not induce a native conformation in the absence of Ca^{2+}. While two specific Gd^{3+}-binding sites were identified in rLB1 in the presence of Ca^{2+}, these sites, defined by the disappearance of resonances Asp4, Glu7, Glu10, Cys18, and Ser20 (site 1, located at the base of the β-hairpin) and Glu40, Ser44, and Thr46 (site 2, located at the C-terminus), are thought not to correspond to the high-affinity calcium site because of the low conservation of affected residues: only Glu10 is conserved across the seven ligand-binding repeats. In the absence of Ca^{2+}, the titration of up to 0.33 molar equiv of Gd^{3+} resulted in the progressive broadening of multiple resonances with no evidence to indicate that the Gd^{3+} was inducing the native fold in rLB1.

Changes were observed in the amide proton chemical shifts on addition of up to an 8-fold molar excess over peptide of diamagnetic cadmium ions; however, the significantly downfield shifted amide resonances characteristic of the native fold were not observed. The inability of Cd^{2+} to induce the native fold in rLB1 suggests that the ion-binding site is more stringently defined than in the EF hand (*20*) and the α-lactablumin elbow (*21*) motifs, where cadmium readily substitutes. The present finding is consistent with studies on the ligand-binding activity of the calcium-dependent LRP, where a selection of divalent ions, including cadmium and manganese, and the trivalent lanthanide ion did not facilitate ligand binding (*9*).

Identification of Potential Calcium Ligands. Seven or eight oxygen atoms are normally involved in the coordination of calcium in proteins, provided by side-chain and backbone atoms from the protein and also from water. Particular

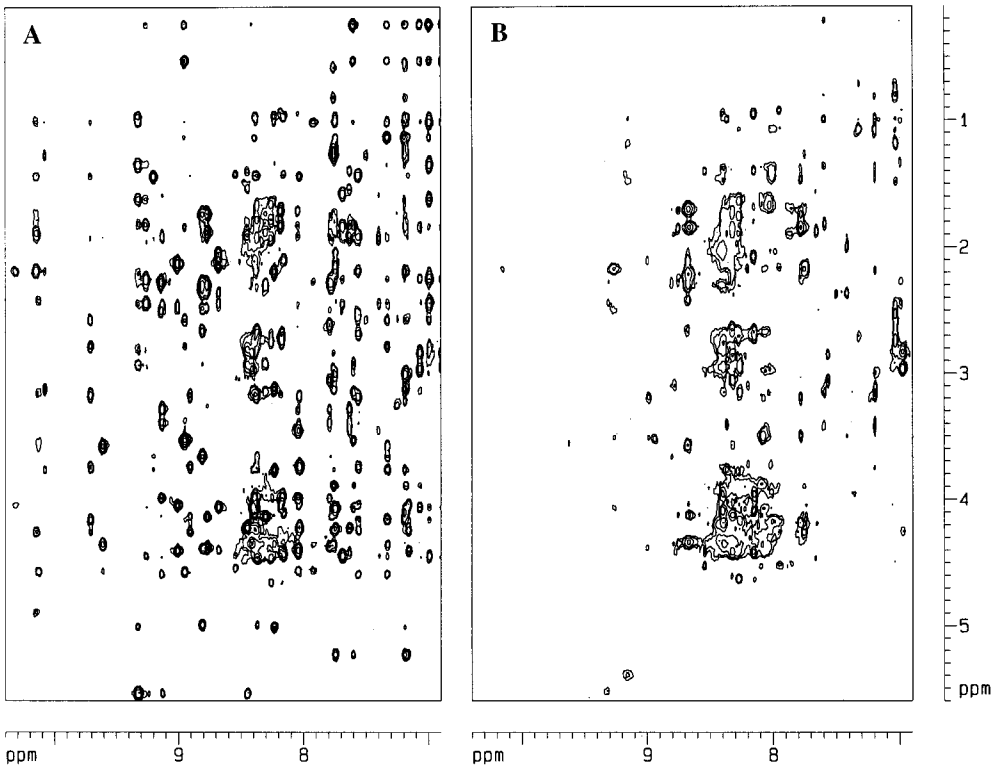

FIGURE 5: The effect of calcium binding on the ^{1}H NMR spectra of rLB1. NOESY spectra were recorded on a ~1.2 mM solution of rLB1 at pH 6.3, 300 K on a Bruker DRX 500 spectrometer in the presence of (A) ~10 mM Ca^{2+} and (B) 1 mM EDTA.

carboxylates involved in ligating the metal ion can, in principle, be identified by monitoring the changes in the chemical shifts of the β protons of Asp and the γ protons of Glu with pH. Completely solvent exposed carboxylic acid side chains are expected to have pK_a values similar to those found in random coil structures (Asp, ~4.0, and Glu, ~4.5), whereas those involved in intra- or intermolecular interactions may have abnormal pK_a's. In this way, groups buried in the core of the protein or involved in salt bridges or metal coordination can be identified.

The titration behavior of the carboxylate β and γ protons of rLB1 was recorded from pH 4.0 to 6.9; spectra could not be recorded at lower pHs because of the denaturation of the peptide. The average chemical shift changes measured over this range were 0.10 ± 0.08 ppm for the β aspartate protons and 0.06 ± 0.03 ppm for the γ glutamate protons. These changes are similar to those reported for human thioredoxin over the pH range 2.1−10.6 (*22*). Although the rLB1 titration curves are incomplete, the β protons of Asp4 and Asp15 and the γ protons of Glu7, Glu10, and Glu30 were seen to readily titrate, implying that these carboxylate groups are solvent-exposed (Figure 7). In contrast, the chemical shifts of the β protons of Asp33 and Asp36 and the γ protons of Glu37 were relatively insensitive to pH changes, consistent with these side chains being protected from free exchange with the solvent.

The two β protons of Asp26 showed different sensitivity to pH changes, the chemical shift of the β proton being relatively insensitive to pH (chemical shift change of only 0.03 ppm) while the β' proton shifted 0.10 ppm. Similarly, the γ' and γ protons of Glu40 moved 0.02 and 0.07 ppm, respectively. This differential sensitivity of geminal protons is unlikely to be the result of the deprotonation of the vicinal carboxylic acid, whose effect must be equal on both protons. Rather, it is proposed that the protons experience a change in environment resulting from the titration of a nearby carboxylic acid.

As mentioned above, the electrostatic changes associated with the titration of acidic side chains in folded proteins affect the electronic environment, and thereby the chemical shift, of nearby nuclei. Thus, protons close to a carboxylate group can function as probes of its ionization state. Amide protons are sensitive probes as the amide bond is more easily polarized than the carbon−proton bond.

The titration curves of all amide protons that move >0.1 ppm were plotted (see Supporting Information), and the pK_{app} values, determined by fitting each curve to the Henderson−Hasselbalch equation, are listed in Table 1. The observed amide titrations were attributed to individual carboxylate groups on the basis of a comparison of the pK_{app} with the pK_a values determined from the proximal protons of the carboxylates, and the distances between titrating groups and amide protons, as measured from the 20 calculated low-energy structures derived from the NMR distance constraints (*1*). The pK_{app} value of the amide of Asp26 of 4.77 ± 0.04 is within experimental error of the values determined for Glu10 and Glu30; the observed titration is attributed to Glu30, however, because of its closer proximity in the solution structures. The relatively small chemical shift changes observed in the β protons of Asp26 can also be attributed to the close proximity of the carboxylate of Glu30. Similarly, the titration of the amide and β protons of Asp33 can be attributed to the carboxylate of Asp15. Of the amide proton titrations observed, only five resonances displayed intrinsic, upfield shifts on titration; the remaining 11 amide resonances moved downfield, consistent with their involvement in transient hydrogen bonds with the titrating carboxylic acid (*23*). The magnitidue of the amide proton shifts of ~0.2

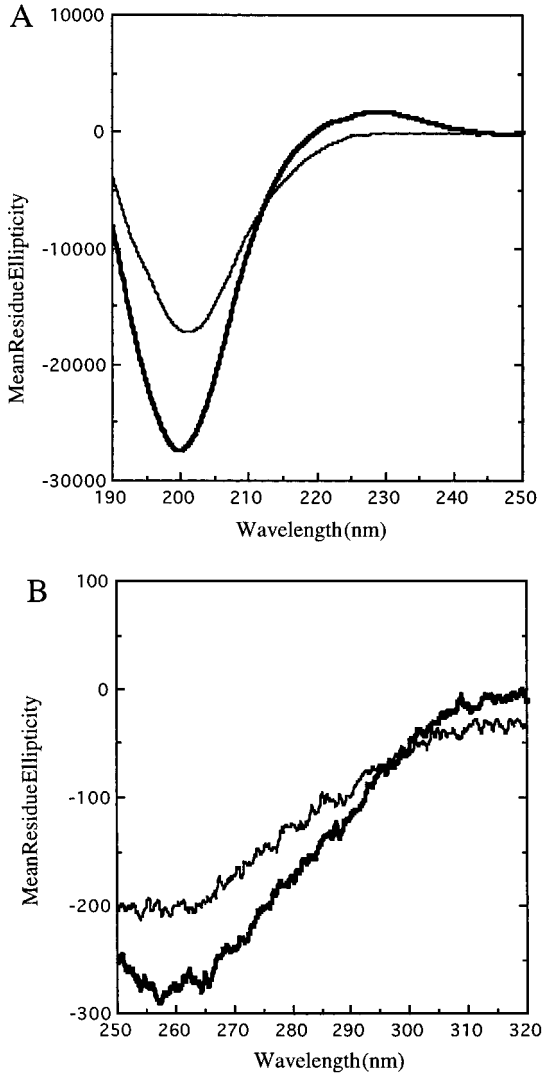

FIGURE 6: Effects of calcium binding on the CD spectra of rLB1: (A) the far-UV spectrum recorded with 30 μM rLB1 and (B) the near-UV spectrum recorded with 230 μM rLB1, at pH 6 and 1 mM Ca^{2+} (thick line), and at pH 3 and 1 mM EGTA (thin line). Results are reported as mean residue ellipticities in units of degrees·cm^2·dmol^{-1}.

ppm suggests that such hydrogen-bonding interactions are weak and will not be seen in calculated structures.

The experimental lower limit for the pH titration curves is pH ~4.0; spectra recorded below this had poorly dispersed resonances, as seen in the spectra recorded in the absence of calcium. This denaturation around pH ~4 is presumably due to the titration of acidic groups coordinating the calcium and further implies that residues 26, 33, 36, 37, and 40 are potentially involved in binding the metal ion. However, Glu40 is not conserved across the LDL repeats and is therefore not expected to be involved in a generic calcium coordination site. An inspection of the NMR-determined structures of rLB1 shows that the side chains of Asp26, Asp36, and Glu37 are sufficiently close to potentially coordinate a calcium ion, while the side chain of Asp33 is ~10 Å away and therefore unlikely to be involved.

Table 1: Titration Parameters for Amide Protons with Shifts Exceeding 0.1 ppm and the Side-Chain Protons of Glu and Asp[a]

residue	proton	p$K \pm 2.5\sigma$	titrating group[b]
Asp4	β	4.24 ± 0.1	Asp4
	β'	4.28 ± 0.1	Asp4
Glu7	HN	4.78 ± 0.07	Glu10
	γ	4.47 ± 0.1	Glu7
	γ'	4.18 ± 0.17	Glu7
Arg8	HN	4.36 ± 0.06	Glu7
Asp15	HN	4.21 ± 0.07	Asp15
	β	4.18 ± 0.04	Asp15
	β'	4.09 ± 0.05	Asp15
Lys17	HN	4.12 ± 0.05	Asp15
Trp23	HN	4.61 ± 0.09	Glu30
Val24	HN	4.68 ± 0.1	Glu30
Asp26	HN	4.77 ± 0.04	Glu30
	β'	4.64 ± 0.09	Glu30
Gly27	HN	4.78 ± 0.03	Glu30
Ala29	HN	4.78 ± 0.05	Glu30
Glu30	HN	4.65 ± 0.03	Glu30
	γ'	4.82 ± 0.08	Glu30
Cys31	HN	4.75 ± 0.06	Glu30
Gln32	HN	3.91 ± 0.04	Asp15
Asp33	HN	3.98 ± 0.08	Asp15
Glu40	HN	4.47 ± 0.03	
	γ'	4.92 ± 0.17	

[a] pK values reported for curve fits where $R^2 > 0.97$. [b] Titrating group identified on the basis of the pK values and the distances between the protons and carboxylate groups, as measured from the NMR structures.

DISCUSSION

Extracellular calcium-binding proteins have been implicated in a range of biological processes: the roles of these proteins in the comparatively calcium rich extracellular milieu appear as varied as for cytoplasmic calcium-binding proteins (*24*), ranging from cell adhesion to calcium sensing and homeostasis (*25*). The calcium-binding, cysteine-rich repeats of the LDL receptor superfamily are independently

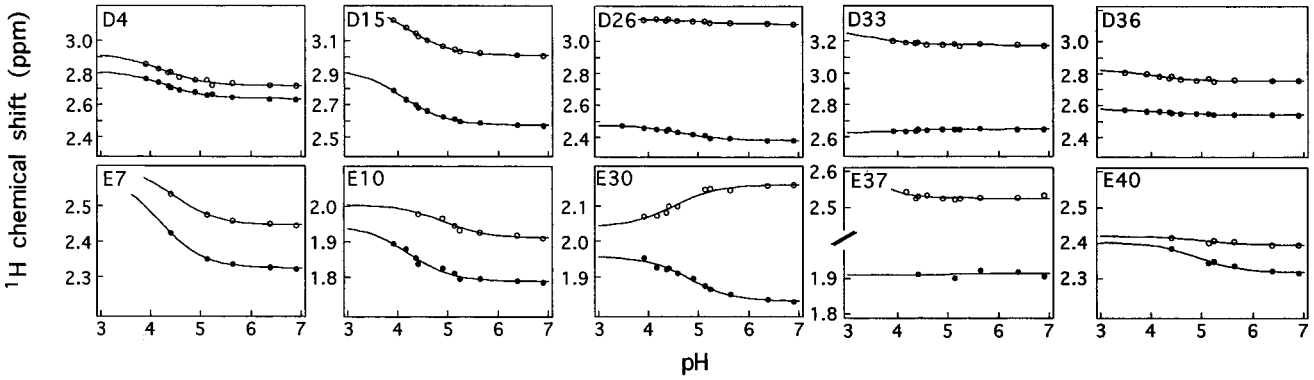

FIGURE 7: pH titration curves for the $\beta\beta'$ protons of aspartic and the $\gamma\gamma'$ protons of glutamic residues. The fit of the data to the Henderson−Hasselbalch equation is shown as the solid line.

FIGURE 8: Stereoview of the superposition of the backbone atoms of the average of the 20 solution structures of LB1 (thick line) on the crystal structure of LB5 (thin line). (A) Superposition of residues 6−37 of LB1 over residues 5−36 of LB5. Only residues 1−37 and 4−36 of LB1 and LB5, respectively, are shown for clarity. (B) The superposition of the calcium-binding loop of LB1 (residues 22−37) on LB5 (residues 21−36). The side chains of LB5 involved in coordination of the calcium ion are shown.

folding domains, in which the dual actions of the calcium and the three intramolecular disulfide bonds produce a peptidic framework that may tolerate a wide range of environments.

The LDLR repeats are not equally involved in the binding of protein ligands. Early mutational studies showed that repeats 3 to 7 were necessary for the binding of the LDL particle (i.e., recognition of apoB-100), whereas repeat 5 is critical for recognition of the β-VLDL (i.e., apoE binding) (*26*). Deletion of the first two repeats in a mutant LDLR has, however, recently been shown to eliminate binding to LDL and β-VLDL (*27*). Furthermore, it has been demonstrated that the LDLR also binds to the receptor-associated protein (*28*) and to lipoprotein lipase (*29*). The binding of several ligands to LRP has been mapped to the second cluster of cysteine-rich repeats and the amino-terminal flanking epidermal growth factor repeat, where overlapping, but discrete, sites were defined for the different ligands. Thus, it is likely that the binding of each of the LDLR ligands involves interaction with discrete repeats or groups of repeats in the ligand-binding domain.

We have shown an unusual ion-binding specificity for the first repeat; rLB1 does not bind Cd^{2+} or Gd^{3+} even though they have comparable ionic radii to Ca^{2+}. A similar ion specificity has been observed for LRP, in which calcium has been proposed to induce a conformational change required for ligand binding; strontium and barium were able to facilitate ligand binding, albeit at higher ion concentrations, but a selection of other divalent ions including cadmium and manganese, and the trivalent lanthanide ion, did not facilitate ligand binding (*9*). In the EF hand, the ion specificity is associated with the ligand at position 12, with Asp allowing binding of both calcium and the smaller magnesium (0.76 Å), whereas Glu makes the site calcium-specific (*30*). Other calcium-binding proteins show less discrimination: the calcium-binding loop of α-lactalbumin can accommodate a range of radii and charges of the coordinating ions, and although a selection of lanthanide ions is able to emulate calcium in inducing structural perturbations, the conformation appears sensitive to the nature of the ion (*18*).

Table 2: Superposition of the Solution Structures of rLB1 and LB5[a]

residues LB1[b]	residues LB5[b]	rmsd (Å)[c]
6−37	5−36	2.20
6−26	5−25	1.22
21−39	20−38	2.17

[a] The 20 lowest energy solution structures of LB1 were superimposed on the crystal structrure of LB5 over the backbone heavy atoms. [b] The portions of the structures over which the structures were superimposed. Residues are numbered as in Figure 1. [c] The reported rmsd values are the averages of the values determined for each solution structure.

During the preparation of this manuscript, the crystal structure of the fifth LDLR repeat was published (*11*), showing an overall fold very similar to that determined for rLB1. The N-terminal β-hairpin structure is well-conserved across the two repeats; however, differences are evident in the C-terminal structure, particularly in the loop apposing the β-hairpin. A superposition of the two-folds is shown in Figure 8A and a comparison of the root-mean-square deviations given in Table 2.

In LB5, a single calcium is coordinated with octahedral geometry by the side chain carboxylates of Asp25, Asp29, Asp35, and Glu36 and the backbone carbonyls of Trp22 and Gly27 (Figure 1). As expected, given the requirement for calcium in these modules, the coordinating acidic side chains identified in the crystal structure are conserved across the

Table 3: Hydrogen Bond Stabilization of the Calcium-Binding Loop

LB5 hydrogen bonds[a]		
donor	acceptor	LB1[b] donor
W22 NH	H19 O	W23NH
R23 NH	S20 O	V24NH
C24 NH	D35 O	C25NH
D25 NH	E36 OE	D26NH
G26 NH	E36 OE	G27NH
G27 NH	D25 OD	S28NH
D29 NH	D35 OD	E30NH
C30 NH	D35 OD	C31NH
K33 NH	C30 O	
S34 NH	D32 OD	
D35 NH	D35 OD	D36NH
E36 NH	K33 O	E37NH
S37 NH	S34 O	38NH

[a] Hydrogen bond donors and acceptors identified in the crystal structure of the calcium-binding loop of LB5 using the Insight program. [b] Slow-exchange amide protons identified in LB1 from deuterium exchange experiments (*1*).

LDLR repeats. The predicted ligands for the calcium in LB1 are therefore the side-chain carboxylates of Asp26, Glu30, Asp36, and Glu37 and the backbone carbonyls of Trp23 and Ser28. The observed insensitivity of the side-chain protons of Asp26, Asp36, and Glu37 to pH changes is consistent with this prediction. However, the side-chain γ protons of Glu30 in rLB1 titrate, indicating that the Glu30 carboxylate is not sequestered from the solvent through calcium coordination. LB1 is unique in that it is the only one of the seven repeats of the LDLR to have a Glu rather than Asp at the position of the second ligating side chain, and it appears that this conservative substitution is not tolerated within the confines of the calcium coordination loop. The observed titrations of seven amide protons within the calcium-binding loop with the carboxylate of Glu30 indicate that this side chain is orientated in toward the calcium loop for potential coordination; thus, steric effects due to the extra methylene presumably prevent its coordination to the metal ion. It is expected that the coordination geometry defined in the crystal structure of LB5 will be maintained in LB1 through the acquisition of a water molecule as the sixth ligand. This loss of one of the peptide ligands in rLB1 provides an explanation for the significantly lower calcium-binding affinity measured for rLB1 compared with LB5 (K_d = 10 μM for rLB1 and 70 nM for LB5).

In the calcium-binding loop of LB5 there is an extensive network of hydrogen bonds, involving backbone amide protons and backbone and side-chain oxygens (Table 3), which appear to stabilize the ion coordination loop similarly to the H-bonding network of the EF hand (*31*). The amide protons involved in hydrogen bonds in LB5 correspond closely to the amide protons found in rLB1 to be in slow exchange with the solvent (Table 3) (*1*), suggesting that the hydrogen-bonding network is maintained in LB1. Thus, the geometry of the calcium-binding loop appears to be preserved in rLB1, despite the loss of the Glu30 ligand (Figure 8B).

Additional hydrogen bonds required to stabilize the tertiary structure were identified in the crystal structure of LB5 between residues at the top of the β-hairpin and apposing residues from the calcium-binding loop. These bonds involve both carboxylate oxygens of Asp32 and Glu16 and the side chain hydroxyl of Ser14. Asp32 is conserved across the ligand-binding repeats of the LDLR, although there is an Asp-to-Asn substitution in LB2, consistent with its proposed crucial role in stabilizing the tertiary structure. In accord with this proposal, the side-chain β protons of the equivalent residue in rLB1, Asp33, do not titrate across the pH range studied. Furthermore, the titration curves of the amide protons of Asp33 and Gln32 indicate the existence of transient hydrogen bonds with the carboxylate of Asp15, evidence of close apposition of these residues. However, Glu16 and Ser14, despite being conserved in LB5 across species, are not conserved across repeats within the LDLR; hence their involvement in essential hydrogen-bonding interactions cannot be extrapolated to the other repeats.

The high degree of conservation of the coordinating residues within the calcium-binding loop, not only in the LDLR superfamily but also in most instances of these repeats, argues that the loop represents a conserved binding motif. The prevalence of mutations within the coordinating loop associated with familial hypercholesterolemia suggests that the coordination geometry is precisely controlled within this motif. In LB5, the mutation of Asp35 to Glu results in incorrect folding of the repeat, as does the nonconservative Asp29 to Gly mutation (*10*). The conservation of all coordinating residues is, however, not essential: the residue equivalent to LB5 Asp29 in LB1, Glu30, does not bind to calcium, but the repeat retains its calcium-binding ability, albeit with lower affinity. It is evident, therefore, that the effect of mutations or substitutions on the ability of repeats to bind calcium depends not only on the position of the coordinating ligand but also on other features inherent in individual repeats.

ACKNOWLEDGMENT

We thank Maria Calderia for expert technical assistance.

SUPPORTING INFORMATION AVAILABLE

pH titration curves for the amide protons found to be sensitive to pH (1 page). Ordering information is given on any current masthead page.

REFERENCES

1. Daly, N. L., Scanlon, M. J., Djordjevic, J. T., Kroon, P. A., and Smith, R. (1995) *Proc. Natl. Acad. Sci. U.S.A. 92*, 6334−6338.
2. Bieri, S., Djordjevic, J. T., Daly, N. L., Smith, R., and Kroon, P. A. (1995) *Biochemistry 34*, 13059−13065.
3. Bieri, S., Djordjevic, J. T., Jamshidi, N., Smith, R., and Kroon, P. A. (1995) *FEBS Lett. 371*, 341−344.
4. Daly, N. L., Djordjevic, J. T., Kroon, P. A., and Smith, R. (1995) *Biochemistry 34*, 14474−14481.
5. Kita, T., Brown, M. S., Watanabe, Y. and Goldstein, J. L. (1981) *Proc. Natl. Acad. Sci. U.S.A.* 78, 2268−2272.
6. van Driel, I. R., Goldstein, J. L., Sudhof, T. C., and Brown, M. S. (1987) *J. Biol. Chem. 262*, 17443−177449.
7. Hodits, R. A., Nimpf, J., Pfistermueller, D. M., Hiesberger, T., Schneider, W. J., Vaughan, T. J., Johnson, K. S., Haumer, M., Kuechler, E., Winter, G., and Blaas, D. (1995) *J. Biol. Chem. 270*, 24078−24085.
8. Horn, I. R., Moestrup, S. K., van der Berg, B. M. M., Pannekoek, H., Nieslen, M. S., and van Zonneveld, A. (1995) *J. Biol. Chem. 270*, 11770−11775.
9. Moestrup, S. K., Kaltoft, K., Sottrup-Jensen, L., and Gliemann, J. (1990) *J. Biol. Chem. 265*, 12623−12628.
10. Blacklow, S. C., and Kim, P. S. (1996) *Nat. Struct. Biol. 3*, 758−762.

11. Fass, D., Blacklow, S., Kim, P. S., and Berger, J. M. (1997) *Nature 388*, 691−693.
12. Djordjevic, J. T., Bieri, S., Smith, R., and Kroon, P. A. (1996) *Eur. J. Biochem. 239*, 214−219.
13. Bax, A., and Davis, D. G. (1985) *J. Magn. Reson. 65*, 355−360.
14. Jeener, J., Meier, B. H., Bachmann, P., and Ernst, R. R. (1979) *J. Chem. Phys. 71*, 4546−4553.
15. Piotto, M., Saudek, V., and Sklenár, V. (1992) *J. Biomol. NMR 2*, 661−665.
16. Ma, L., and Anderson, S. (1997) *Biochemistry 36*, 3728−3736.
17. Kuhlman, B., Boice, J. A., Wu, W., Fairman, R., and Raleigh, D. P. (1997) *Biochemistry 36*, 4607−4615.
18. Aramini, J. M., Hiraoki, T., Grace, M. R., Swaddle, T. W., Chiancone, E., and Vogel, H. J. (1996) *Biochim. Biophys. Acta 1293*, 72−82.
19. Overduin, M., Harvey, T. S., Bagby, S., Tong, K. I., Yau, P., Takeichi, M., and Ikura, M. (1995) *Science 267*, 386-389.
20. Bjornson, M. E., Corson, D. C., and Sykes, B. D. (1985) *J. Inorg. Biochem. 25*, 141−149.
21. Aramini, J. M., Hiraoki, T., Ke, Y., Nitta, K., and Vogel, H. J. (1995) *J. Biochem. (Tokyo) 117*, 623−628.
22. Forman-Kay, J. D., Clore, G. M., and Gronenborn, A. M. (1992) *Biochemistry 31*, 3442−3452.
23. Szyperski, T., Antuch, W., Schick, M., Betz, A., Stone, S. R., and Wüthrich, K. (1994) *Biochemistry 33*, 9303−9310.
24. Maurer, P., Hohenester, E., and Engel, J. (1996) *Curr. Opin. Cell Biol. 8*, 609−617.
25. Lundgren, S., Hjälm, G., Hellman, P., Ek, B., Juhlin, C., Rastad, J., Klareskog, L., Akerstrom, G., and Rask, L. (1994) *Exp. Cell Res. 212*, 344−350.
26. Russell, D. W., Brown, M. S., and Goldstein, J. L. (1989) *J. Biol. Chem. 264*, 21682−21688.
27. Sass, C., Giroux, L., Lussier-Cacan, S., Davignon, J., and Minnich, A. (1995) *J. Biol. Chem. 270*, 25166−25171.
28. Medh, J. D., Fry, G. L., Bowen, S. L., Pladet, M. W., Strickland, D. K., and Chappell, D. A. (1995) *J. Biol. Chem. 270*, 536−540.
29. Medh, J. D., Bowen, S. L., Fry, G. L., Ruben, S., Andracki, M., Inoue, I., Lalouel, J., Strickland, D. K., and Chappell, D. A. (1996) *J. Biol. Chem. 271*, 17073−17080.
30. da Silva, A. C. R., Kendrick-Jones, J., and Reinach, F. C. (1995) *J. Biol. Chem. 270*, 6773−6778.
31. Strynadka, N. C. J., and James, M. N. G. (1989) *Annu. Rev. Biochem. 58*, 951−998.
32. Dirlam, K. A., Gretch, D. G., LaCount, D. J., Sturley, S. L., and Attie, A. D. (1996) *Protein Expression Purif. 8*, 489−500.

BI972529N